Effects of Solute Nb Atoms and Nb Precipitates on Isothermal Transformation Kinetics from Austenite to Ferrite

LI WANG, SALLY PARKER, ANDREW ROSE, GEOFF WEST, and RACHEL THOMSON

Nb is a very important micro-alloying element in low-carbon steels, for grain size refinement and precipitation strengthening, and even a low content of Nb can result in a significant effect on phase transformation kinetics from austenite to ferrite. Solute Nb atoms and Nb precipitates may have different effects on transformation behaviors, and these effects have not yet been fully characterized. This paper examines in detail the effects of solute Nb atoms and Nb precipitates on isothermal transformation kinetics from austenite to ferrite. The mechanisms of the effects have been analyzed using various microscopy techniques. Many solute Nb atoms were found to be segregated at the austenite/ferrite interface and apply a solute drag effect. It has been found that solute Nb atoms have a retardation effect on ferrite nucleation rate and ferrite grain growth rate. The particle pinning effect caused by Nb precipitates is much weaker than the solute drag effect.

DOI: 10.1007/s11661-016-3548-x

I. INTRODUCTION

DURING steel manufacturing, many alloying elements are added for various purposes. Nb is one of the most important micro-alloying elements in low–carbon steels. The large misfit between Nb atoms and the austenite matrix makes the solubility of Nb in austenite low, and thus the Nb content in low-carbon steels is normally quite low, *i.e.*, less than 0.05 wt pct. Nb has a strong tendency to form a carbo-nitride, and thus there are two typical forms of Nb present in steels during steel manufacturing, which are solute Nb atoms and Nb carbo-nitride precipitates.[1–5] Nb addition in steels is beneficial for mechanical properties by grain size refinement and precipitation strengthening. Nb can also be used to control the transformation kinetics, and thus hardenability is improved by the presence of solute Nb.[1–7]

The effects of Nb on steel manufacturing have been studied widely by many researchers. Many of them state that Nb has a retardation effect on phase transformation kinetics in steels,[6–18] and even a small amount of Nb (*i.e.*, less than 0.05 wt pct) can result in significant effects on transformation behavior and mechanical properties. The presence of Nb in steels also affects the final microstructure after phase transformations.[18] However, the effects of Nb on isothermal transformation kinetics from austenite to ferrite have not yet been fully characterized and quantified. In particularly, the two forms of Nb in steels, solute Nb atoms and Nb precipitates, can affect phase transformation kinetics *via* different mechanisms, which are the solute drag effect and particle pinning effect. Since there is still controversy about the exact nature of the retardation mechanism,[7,16] advanced microscopy techniques can be utilized for samples with different heat treatments to characterize the solute drag effect and the particle pinning effect. The solute drag effect has been demonstrated by many previous researchers.[19–23] Its basic requirement is the segregation of solute atoms to the transformation interface, and thus the grain boundary mobility is inhibited. Felfer *et al.*[23] have utilized atom probe study to find that the interfacial excess Nb atoms at prior austenite grain boundaries are more than those at ferrite-ferrite grain boundaries. Fazeli and Militzer[24] have successfully studied the solute drag effect in Fe-C-Mn ternary system, but the solute drag effect caused by Nb has not yet been fully understood. Nb carbo-nitride particles are quite small (typically tens of nanometers) after typical heat treatments in steels. The combination of the small particle size and the low content of Nb make it difficult to observe Nb precipitates.

Austenite grain growth, which has a significant effect on the subsequent transformation kinetics, is also affected by the presence of Nb. In order to accurately study the effects of Nb on transformation behavior, it is

LI WANG, formerly PhD student with the Department of Materials, Loughborough University, Loughborough LE11 3TU, UK, is now Engineer with Jaguar Land Rover, Coventry. Contact e-mail: liwangmaterials@outlook.com SALLY PARKER, Principal Research Metallurgist, and ANDREW ROSE, Principal Investigator, are with the Materials Design Department, Tata Steel R\&D, Swinden Technology Centre, Rotherham S60 3AR, UK. GEOFF WEST, formerly Research Fellow with Loughborough University, is now Senior Research Fellow with the University of Warwick, Coventry, UK. RACHEL THOMSON, Professor, is with the Department of Materials, Loughborough University.

Manuscript submitted September 2, 2015.
Article published online May 2, 2016

important to isolate the effects of austenite grain size, solute Nb atoms, and Nb precipitates. Nucleation and ferrite grain growth are the two stages in a typical reconstructive transformation from austenite to ferrite. It is essential to study nucleation rate and grain growth rate separately for fully understanding the effects of Nb on transformation kinetics.

II. EXPERIMENTAL PROCEDURE

Five laboratory-cast low-carbon steels with the same base chemistry but different Nb contents were provided by Tata Steel, and their chemical compositions are listed in Table I. Steels 1 to 3 are from the same batch, but steels 4 and 5 are from another batch with different initial processing conditions.

Samples were cut into cylinders with a length of 10 mm and a diameter of 5 mm for dilatometer operation. A dilatometer (DIL 805A/D) was utilized for heat treatments and recording transformation kinetics. ThermoCalc in conjunction with the TCFE v6 database was utilized for thermodynamic calculations of the precipitate dissolution and phase transformation temperatures (Table I) which were used to determine appropriate heat treatment temperatures. The heat treatment temperature profiles are shown in Figure 1. Samples were fast heated to 1523 K (1250 °C) to transform to austenite and fully dissolve pre-existing Nb precipitates, and holding times were varied for different steels in order to make all the samples with the same average prior austenite grain size. They were then fast cooled to 1173 K (900 °C) and held for a certain time (*i.e.*, 5, 20, or 60 minutes) to allow Nb carbo-nitride precipitation to occur. After that, they were fast cooled to isothermal transformation temperatures between 1023 K (750 °C) and 923 K (650 °C), and held for 10, 30 seconds, 1, 2, 3, or 15 minutes. Finally, the samples were quenched to room temperature. Some samples were fast cooled directly from 1523 K (1250 °C) to the isothermal transformation temperatures without the precipitation holding at 1173 K (900 °C), in order to retain Nb atoms in solid solution at the beginning of the isothermal transformation. A sample was quenched directly from 1523 K to room temperature in order to analyze whether Nb carbo-nitride particles can be formed during the fast cooling. Additional samples were austenitized at 1373 K (1100 °C) for a certain time, in order to avoid the complete dissolution of pre-existing Nb precipitates, before undergoing isothermal transformations as before.

After the heat treatments, the samples were prepared using standard metallurgical preparation methods including cutting, mounting, grinding, polishing, and sometimes chemical etching with 2 pct Nital. A Reichert-Jung MEF3 reflective optical microscope, a Zeiss 1530VP field emission gun scanning electron microscope (FEGSEM), an FEI Nova 600 NanoLab dual beam system which consists of FEGSEM and a gallium source focused ion beam (FIB), a JEOL 2000FX transmission electron microscope (TEM) equipped with an Energy-Dispersive X-ray (EDX) detector, and an FEI Tecnai F20 field emission gun transmission electron microscope (FEGTEM) fitted with high angle annular dark field (HAADF) detector and X-Max 80 mm SDD detector were utilized to investigate the resulting microstructures.

III. EFFECTS OF SOLUTE NB ATOMS ON ISOTHERMAL TRANSFORMATION

In order to study the effect of solute Nb atoms on transformation kinetics, steels 1 to 3 with similar chemical compositions except for the Nb content were heated to 1523 K (1250 °C) to ensure that all pre-existing Nb(C,N) precipitates were fully dissolved. From thermodynamic calculation, the solubility of Nb at 1523 K for a steel with 0.1 wt pct C is 0.09 wt pct. The austenitization times were carefully chosen to obtain an average prior austenite grain size of ~80 μm in each sample. Therefore, the subsequent isothermal transformation should only be affected by any difference in solute Nb atoms.

The transformation kinetics curves of steels 1 to 3 during 15-minute isothermal transformations at 1023 K (750 °C), 998 K (725 °C), 973 K (700 °C), 948 K (675 °C), and 923 K (650 °C) are plotted in Figures 2(a) through (e), respectively. It can be clearly observed that steel 3 with 0.028 wt pct Nb always has the slowest

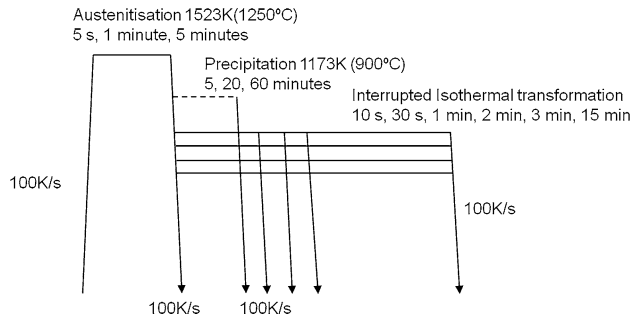

Fig. 1—Temperature profile for interrupted isothermal transformations.

Table I. Chemical Compositions (Weight Percentage) and Thermodynamic Calculation Results

Steel	C	Nb	N	Si	Mn	Al	Ti	Fe	Nb(C,N) Dissolution	Ae_3
1	0.110	<0.001	0.006	0.23	0.99	0.034	0.001	bal	N/A	1117 K (844 °C)
2	0.105	0.009	0.006	0.23	1.00	0.030	0.001	bal	1293 K (1020 °C)	1119 K (846 °C)
3	0.105	0.028	0.006	0.23	0.99	0.031	0.001	bal	1414 K (1141 °C)	1119 K (846 °C)
4	0.088	0.045	0.005	0.23	1.01	0.032	<0.001	bal	1447 K (1174 °C)	1132 K (859 °C)
5	0.096	0.067	0.005	0.23	1.01	0.029	<0.001	bal	1493 K (1220 °C)	1130 K (857 °C)

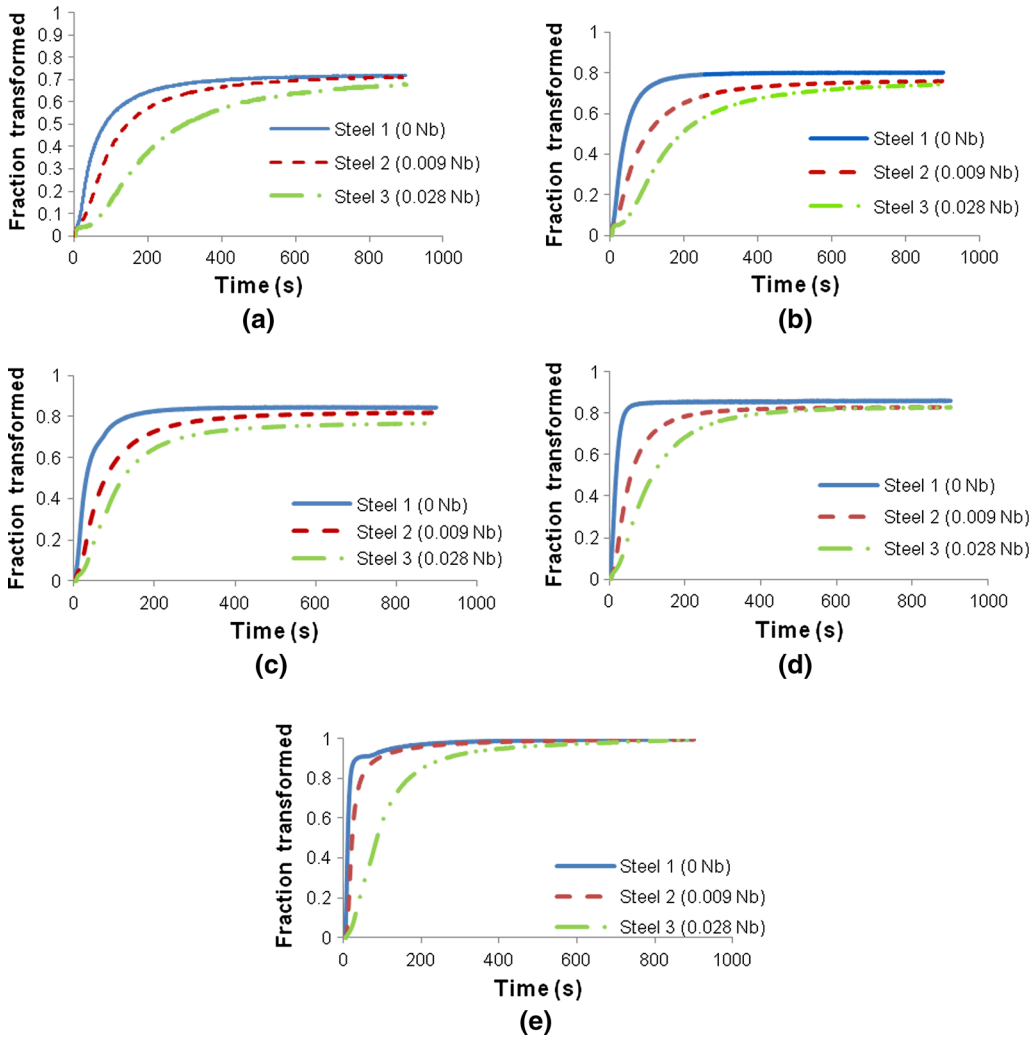

Fig. 2—Isothermal transformation kinetics for steels 1 to 3 with the same prior austenite grain size at (*a*) 1023 K (750 °C), (*b*) 998 K (725 °C), (*c*) 973 K (700 °C), (*d*) 948 K (675 °C), and (*e*) 923 K (650 °C).

transformation kinetics, and steel 1 with no Nb always has the fastest transformation kinetics in the steels. In this temperature range, the isothermal transformations are mainly occurring by the reconstructive mechanism to transform to polygonal ferrite. However, at 923 K (650 °C), from Figure 2(e), it can be found that steel 1 has a 'stasis' after 90 pct transformation, and the transformation restarts after tens of seconds. This phenomenon has also been found by Furuhara *et al.*[25] in upper bainite transformation at 853 K and 873 K (580 °C and 600 °C). From the optical micrographs shown in Figures 3(e) and (f), steels 1 and 3 have different microstructures after the 15-minute isothermal transformations at the same temperature of 923 K (650 °C). Steel 1 has a combination of displacive and diffusional transformation products, but steel 3 was mainly ferrite, pearlite, and martensite. Therefore, their transformation kinetics can not only be directly compared at this temperature, but it also indicates that the presence of Nb has an effect on the competition between diffusional and displacive transformation mechanisms.

All of these isothermal transformation results indicate that a steel with a higher Nb content always has slower isothermal transformation kinetics. The steels were all austenitized at 1523 K (1250 °C) which is much higher than the Nb(C,N) dissolution temperatures. Therefore, the Nb should be in solid solution form at the beginning of the isothermal transformation, and this has been investigated by the TEM carbon extraction replica study on samples quenched directly from 1523 K (1250 °C), in which no Nb(C,N) particles were observed. However, from a TEM carbon extraction replica study on the isothermally transformed samples from steel 3 after quenching directly from 1523 K (1250 °C), there were a lot of Nb(C,N) particles segregated near grain boundaries, as indicated by the arrows in Figure 4. These Nb(C,N) particles are quite small, with a typical diameter of ~10 nm, which is much smaller than that of typical pre-existing Nb(C,N) particles. It is reasonable to suggest that during the isothermal transformations, solute Nb atoms were segregated at grain boundaries where they acted to delay the transformation

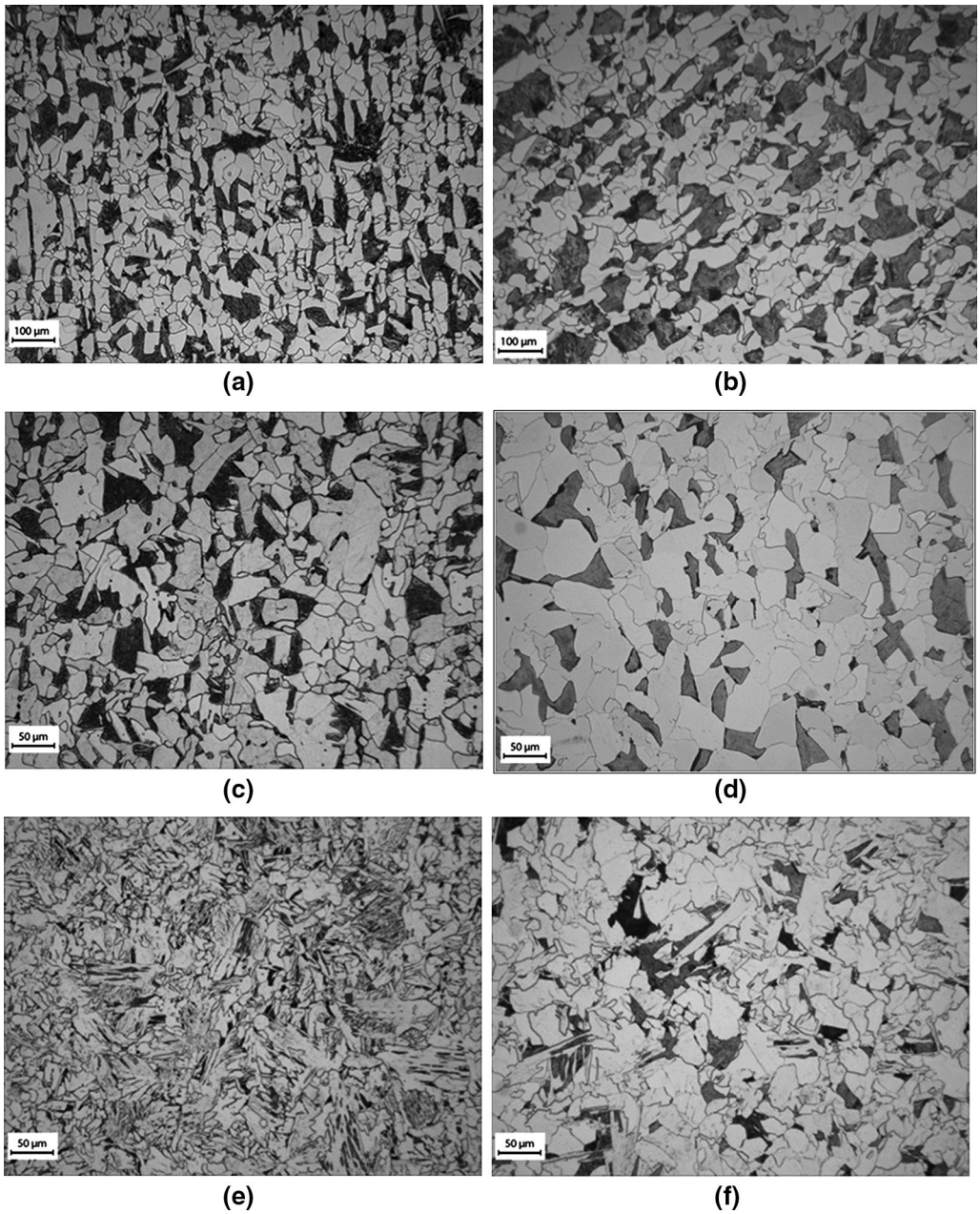

Fig. 3—Optical micrographs of steels 1 and 3 after 15-minute isothermal transformations: (*a*) steel 1 at 1023 K (750 °C), (*b*) steel 3 at 1023 K (750 °C), (*c*) steel 1 at 973 K (700 °C), (*d*) steel 3 at 973 K (700 °C), (*e*) steel 1 at 923 K (650 °C), and (*f*) steel 3 at 923 K (650 °C).

kinetics, and then precipitated as Nb(C,N) particles which were left near the grain boundary during the subsequent isothermal transformation.

IV. INTERRUPTED ISOTHERMAL TRANSFORMATIONS

A typical isothermal transformation from austenite to ferrite has a parabolic kinetic curve. The ferrite nucleation rate and ferrite grain growth rate are the two key factors for the transformation kinetics. In order to accurately study the effect of solute Nb atoms on each rate, the isothermal transformations were interrupted after a certain time and then the samples were quenched to room temperature. For each interrupted sample, the average ferrite grain size was measured using linear intercept method and number of ferrite grains was counted. Ferrite grain sizes during holding at 1023 K (750 °C) for the three steels are plotted in Figure 5(a), and an error bar shows the standard deviation of grain size. The curves of average number of ferrite grains per unit area as a function of holding time for the steels are plotted in Figure 5(b), and an error bar shows the standard deviation of the number of grains per unit area for all the micrographs in a steel.

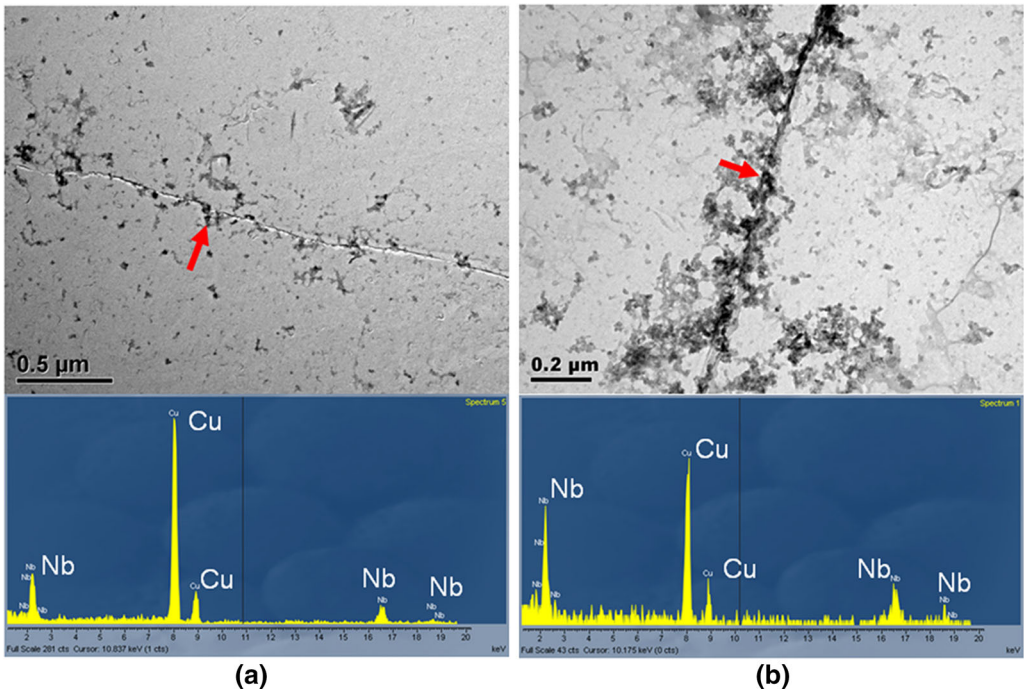

Fig. 4—TEM images and the related EDX spectrum of carbon extraction replica samples from steel 3 after isothermal transformation at (*a*) 923 K (650 °C) and (*b*) 973 K (700 °C).

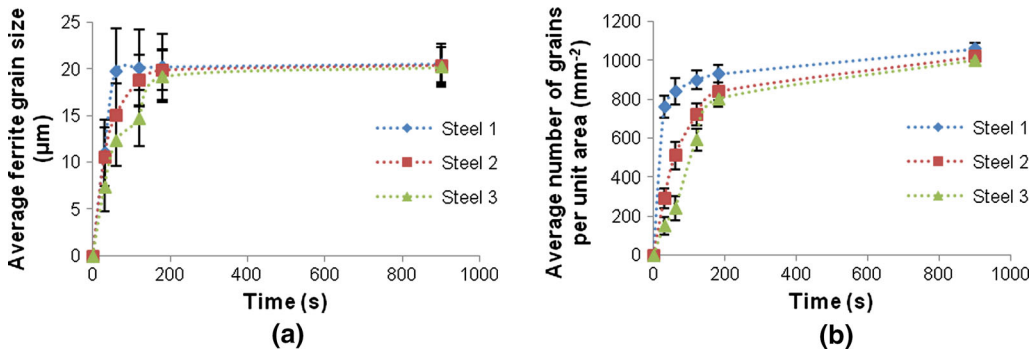

Fig. 5—(*a*) Average ferrite grain size (an error bar shows the standard deviation of grain size and (*b*) average number of ferrite grains per unit area (an error bar shows the standard deviation of the number of grains per unit area for all the micrographs in a steel), during isothermal transformations at 1023 K (750 °C) for steels 1 to 3.

For the Nb-free steel 1, it was found that the number of ferrite grains increased quickly in the first tens of seconds, and the ferrite grain size also grew quickly simultaneously. After that, the ferrite grain size became stable, but there was still a slow increase in the number of ferrite grains. In this work, the nucleation rate is calculated by dN/dt, where N is the number of ferrite grains and t is the time. The ferrite grain growth rate is calculated by dD/dt, where D is the average feret diameter of grains. Compared with the interrupted samples of steel 1, it is clear that the interrupted transformed samples of steel 2 with 0.009 wt pct Nb always had fewer ferrite grains and a smaller average ferrite grain size than samples from steel 1 after 10, 60, and 120 seconds holding at 1023 K (750 °C). However, the nucleation rate and the grain growth rate of steel 3 with 0.028 wt pct Nb were even lower than those of steel 2. When the ferrite grain size of steel 3 achieved a similar level to the final ferrite grain size after 180 seconds, the transformation was still in progress, and more ferrite grains would be formed to increase the total ferrite fraction, but the average ferrite grain size remained constant. These measured data were consistent with the kinetics plot in Figure 2(a). For isothermal transformations at other temperatures between 923 K (650 °C) and 1023 K (750 °C), the nucleation rate and the grain growth rate in steel 3 were always slower than those in steels 1 and 2, and therefore the transformation kinetics for steel 3 is always slower than steels 1 and 2 as shown in Figures 2(b) through (e). Since the only difference among the steels is the Nb content, and Nb atoms were all in solid solution at the beginning of the isothermal

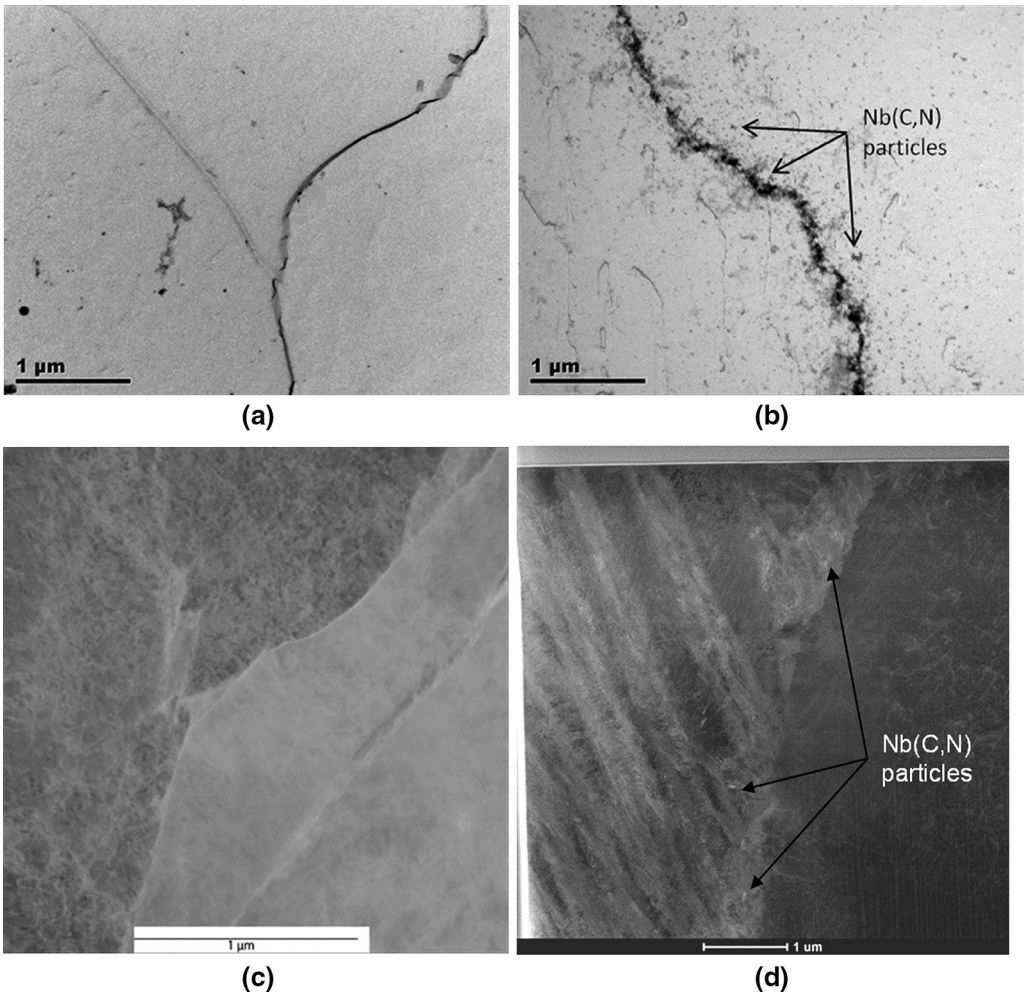

Fig. 6—TEM images for carbon extraction replica samples of steel 3 with (*a*) 60 s or (*b*) 180 s, interrupted isothermal transformations at 1023 K (750 °C), and TEM images for FIB lift out samples of steel 3 with (*c*) 60 s or (*d*) 180 s, interrupted isothermal transformations at 1023 K (750 °C).

transformations, it can be concluded that solute Nb atoms have a retardation effect on both the ferrite nucleation rate and the ferrite grain growth rate.

In order to study the mechanism of the retardation effect caused by solute Nb atoms, the interrupted isothermally transformed samples of steel 3 were characterized using TEM. Figure 6(a) and (b) are the TEM images for carbon extraction replica samples of steel 3 after 60-second or 180-second isothermal transformation at 1023 K (750 °C). After 60 seconds, few Nb(C,N) particles were found. However, many Nb(C,N) particles with a particle size of ~10 nm were seen to be segregated on grain boundaries after 180-second holding at 1023 K (750 °C). Since solute Nb atoms have a lower diffusion coefficient than carbon atoms in both austenite and ferrite,[1] they cannot diffuse to a long distance within 180 seconds at 1023 K (750 °C). Therefore, these TEM images indicate that solute Nb atoms segregate at the transformation interfaces during the isothermal transformation. The solute Nb atoms move with the transformation interface, and thus the interface mobility is reduced. This phenomenon is consistent with the solute drag theory.[21–23] In the carbon extraction replica technique, the matrix has been etched, with only precipitates left on the carbon film, and therefore the density of the precipitates is possibly more than its real value. In order to do a more accurate characterization, a small area across a ferrite/martensite grain boundary was lifted out using FIB, and the microstructure was analyzed using TEM under bright mode or high angle annular dark field (HAADF) mode, as shown in Figures 6(c) and (d). No obvious Nb(C,N) particles can be seen in the sample with 60 second holding, but many small Nb precipitates can be seen in the sample with 180-second holding. From Figure 5(a), the ferrite grain growth rate in steel 3 is much slower than those of steels 1 and 2 up to 180-seconds isothermal transformation at 1023 K (750 °C). Figure 2(a) shows that steels 1 and 2 have much more fraction transformed than steel 3 after 180-second isothermal transformation at 1023 K (750 °C), which can be attributed to the influence of solute Nb atoms.

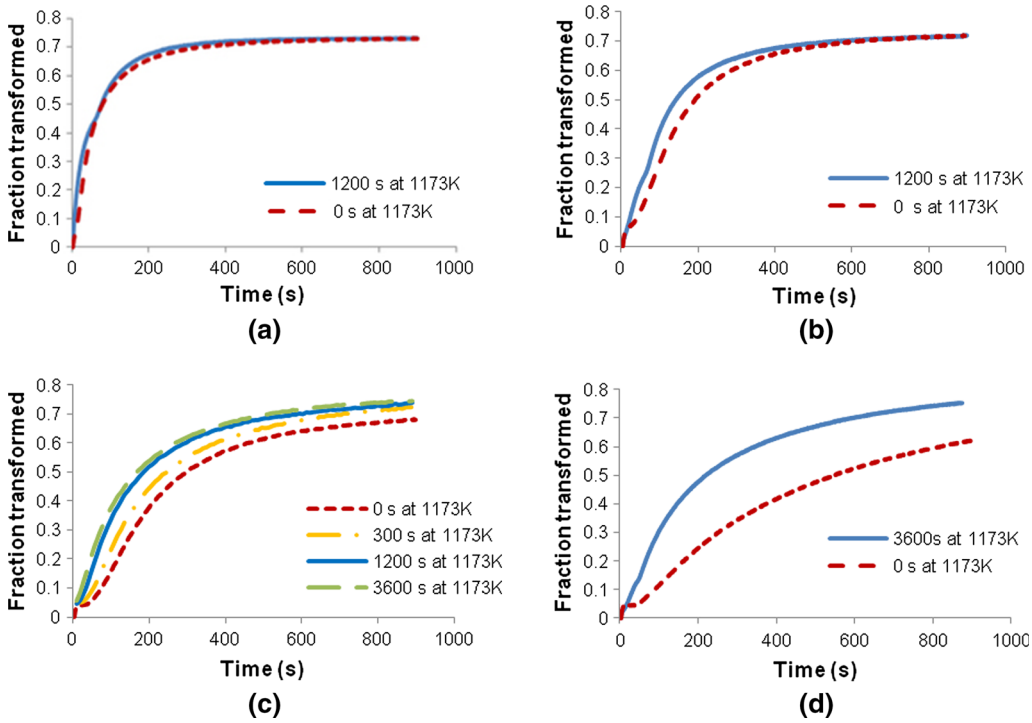

Fig. 7—Isothermal transformation kinetics at 1023 K (750 °C) with or without holding at 1173 K (900 °C) for (*a*) steel 1, (*b*) steel 2, (*c*) steel 3, and (*d*) steel 4.

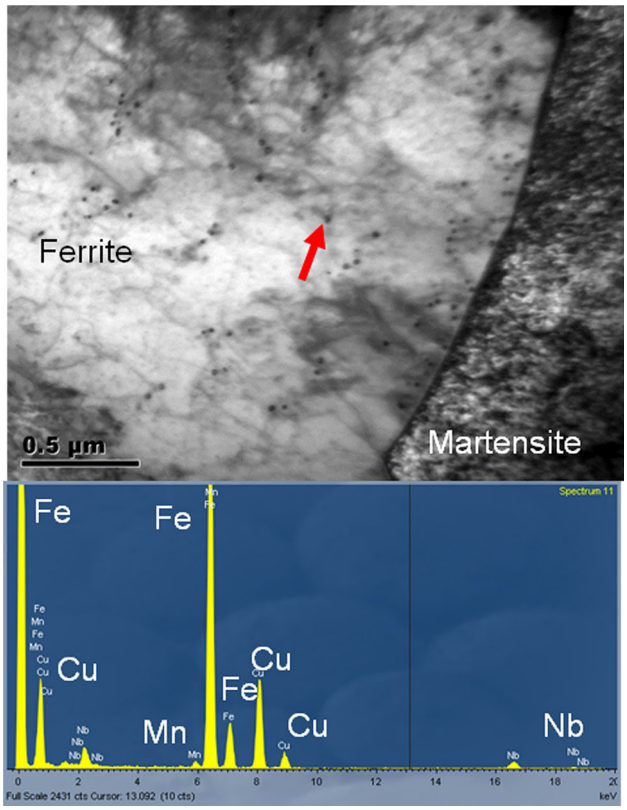

Fig. 8—A TEM image and the related EDX spectrum of a FIB lift out sample of steel 4 with 5-min austenitization at 1523 K (1250 °C) and 1-h holding at 1173 K (900 °C) and then isothermal transformation at 1023 K (750 °C).

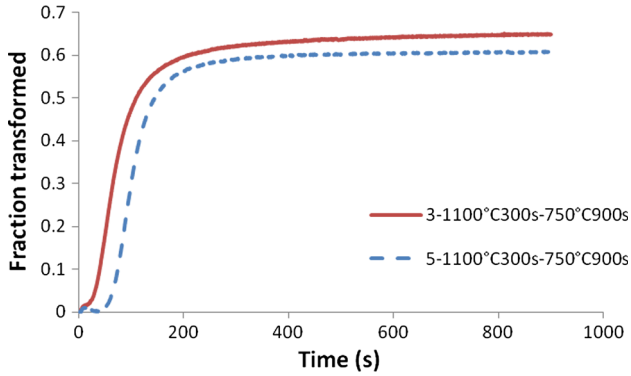

Fig. 9—Isothermal transformation kinetics at 750 °C for steels 3 and 5 with austenitization temperatures below Nb(C,N) dissolution temperature.

V. EFFECTS OF NB PRECIPITATES ON ISOTHERMAL TRANSFORMATION

In order to study the effects of Nb(C,N) precipitates on the transformation behavior, samples were cooled to 1173 K (900 °C) after austenitization at 1523 K (1250 °C), and held for a certain time to allow solute Nb atoms to precipitate as Nb(C,N) particles before the subsequent isothermal transformations. The isothermal transformation kinetics at 1023 K (750 °C) of the four steels with 300-, 1200-, or 3600-second holding at 1173 K (900 °C) or without holding at 1173 K (900 °C) are plotted in Figures 7(a) through (d), respectively. From Figure 7(a), there was a little difference in the transformation kinetics of the samples from steel 1,

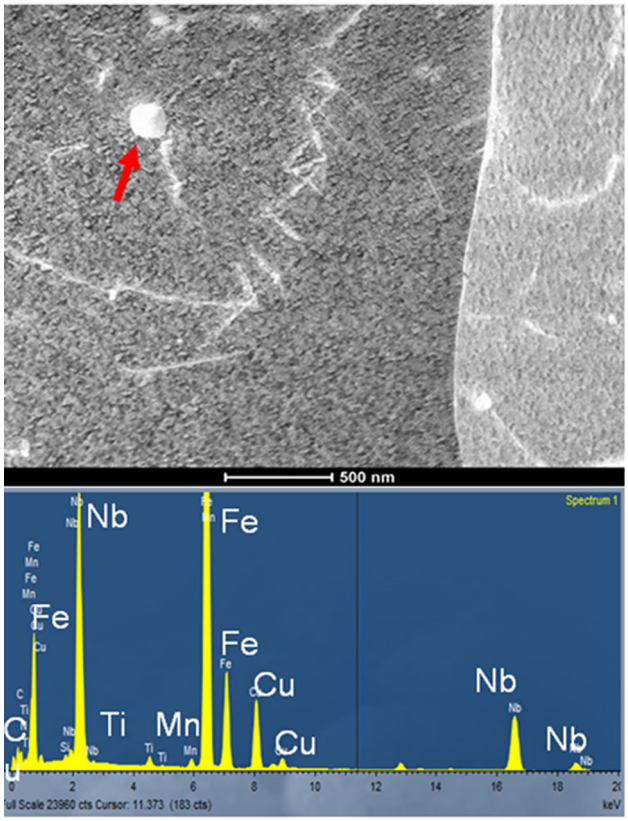

Fig. 10—A TEM image and the related EDX spectrum of a FIB lift out sample of steel 5 with 5-min austenitization at 1373 K (1100 °C) and then isothermal transformation at 1023 K (750 °C).

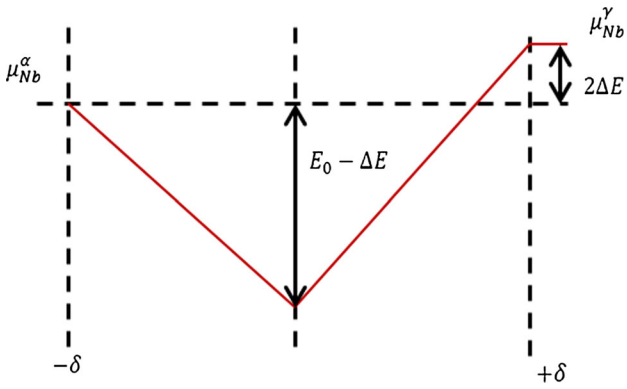

Fig. 11—Schematic diagrams of chemical potential profile across the interface between austenite (γ) and ferrite (α).

because steel 1 is Nb-free, and 1200-seconds holding at 1173 K (900 °C) resulted in little prior austenite grain growth. From Figure 7(b), 1200-second holding at 1173 K (900 °C) slightly accelerated the isothermal transformation kinetics of steel 2, because solute Nb atoms which can delay the transformation kinetics had been precipitated as Nb(C,N) particles during the holding at 1173 K (900 °C). From Figure 7(c), it can be seen that the transformation kinetics became faster with increasing holding time at 1173 K (900 °C) for steel 3. However, there was a little increase in transformation kinetics between the sample with 1200-second holding and the sample with 3600 seconds, possibly because most solute Nb atoms had already been precipitated during 1200-second holding.[2] For steel 4 with 0.045 wt pct Nb, holding at 1173 K (900 °C) for 3600 seconds significantly accelerated the isothermal transformation kinetics at 1023 K (750 °C), as shown in Figure 7(d).

The presence of Nb(C,N) particles in the sample from steel 4 with 1-hour holding at 1173 K (900 °C) and then isothermal transformation at 1023 K (750 °C) was studied using TEM, as shown in Figure 8. From a FIB lift out area across a ferrite/martensite interface, many Nb(C,N) particles were observed, with a high density of dislocations around them. Some Nb(C,N) particles were found near the interface, but there were also many particles away from the interface.

It can be concluded that holding at 1173 K (900 °C) accelerates the subsequent isothermal transformation kinetics. Solute Nb atoms precipitate as Nb(C,N) particles, and thus the solute drag effect is reduced. Nb(C,N) particles can exert a particle pinning effect on the transformation kinetics, but their effect appears to be much weaker than the solute drag effect according to the dilatometry results.

Figure 9 shows the dilatometer curves of isothermal transformation at 1023 K (750 °C) for steels 3 and 5 after the austenitization at a temperature lower than the typical Nb(C,N) dissolution temperatures in order to remain some pre-existing Nb(C,N) particles and analyze their effect on transformation kinetics. Steels 3 and 5 with 5-minutes austenitization at 1373 K (1100 °C) both resulted in an average prior austenite grain size of ~30 μm. It can be seen that although steel 5 has much more Nb content than steel 3, its transformation kinetics is only slightly slower than steel 3.

Figure 10 shows an example of the effect of a pre-existing Nb(C,N) particle on the isothermal transformation at 1023 K (750 °C). The sample was from steel 5 which had undertaken an austenitization heat treatment at 1373 K (1100 °C). After 15-minute isothermal transformation at 1023 K (750 °C), a pre-existing Nb(C,N) particle with the size about 100 nm, which is much larger size than typical Nb(C,N) particles precipitated during the isothermal transformation at 1023 K (750 °C), can be found away from the grain boundary, and no high density of dislocations can be observed around the pre-existing particle. Therefore, It is reasonable to consider that the pre-existing Nb(C,N) particle makes much less contribution to delay transformation kinetics.

VI. DISCUSSION

All of the dilatometer results and microscopy images indicate that solute Nb has a retardation effect on transformation kinetics. For the samples directly quenched from 1523 K (1250 °C) to the isothermal transformation temperatures, it is reasonable to assume all Nb atoms are in solid solution at the beginning of the isothermal transformation, because no Nb(C,N) particles have been found using TEM in samples directly quenched from 1523 K

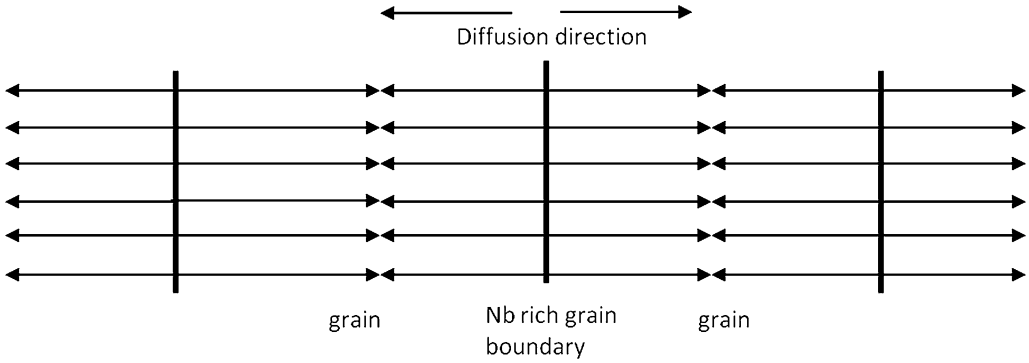

Fig. 12—Schematic diagram of Nb atoms diffusion in steels at a high temperature.

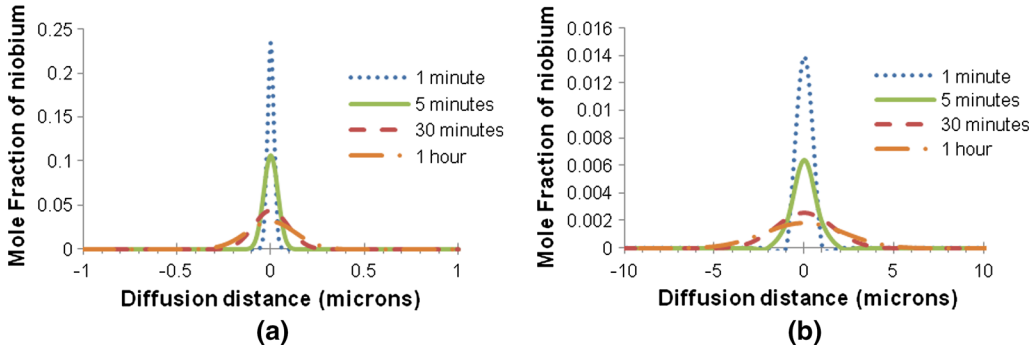

Fig. 13—Nb concentration profiles after various times diffusion at 1023 K (750 °C) from grain boundaries into (*a*) austenite grains and (*b*) ferrite grains, in the system shown in Fig. 11.

(1250 °C) to room temperature. During the isothermal transformations, a steel with a high Nb content was always found to have a slower transformation rate than a steel with a low Nb content, and the delay on transformation kinetics typically happened in the first few minutes. At the beginning, the transformation was delayed by solute Nb atoms, because all the Nb atoms were still in solid solution. Nb atoms have a low solubility in the ferrite lattice, and they prefer to segregate at prior austenite grain boundaries, where a large amount of defects are typically present. As a result, more energy is required for ferrite nucleation.

Even for the nucleated ferrite grains, many solute Nb atoms remain around the interface between the ferrite and austenite, because the newly formed ferrite grains are quite small, and the diffusion of solute Nb atoms in iron matrix is quite slow. Nb is a ferrite stabilizer, and thus the chemical potential of solute Nb atoms in ferrite is lower than that in austenite. In addition, there should be a potential well at the interface to explain the attraction of solute atoms. A schematic diagram of chemical potential across a ferrite/austenite interface is shown in Figure 11, where $\mu_{\mathrm{Nb}}^{\alpha}$ is the interaction energy between solute Nb atoms and ferrite, $\mu_{\mathrm{Nb}}^{\gamma}$ is the interaction energy between solute Nb atoms and austenite, $2\Delta E$is the difference of interaction energy for solute Nb atoms in austenite and ferrite phases, δ is the half width of the boundary between ferrite and austenite, and $E_0 - \Delta E$ is the potential well showing the binding energy of Nb atoms at the boundary.

A brief model can be developed to roughly estimate the diffusion rate of Nb atoms during the phase transformation. For a NbC particle precipitated at a prior austenite grain boundary, it can be assumed that the local Nb mole fraction is 0.5. Although Nb contents in the steels are not high enough to fully fill the prior austenite grain boundaries, it can be assumed that the fastest diffusion case is when some boundaries are full of NbC precipitates and there are no Nb particles inside the grains. However, there are many grain boundaries and the diffusion from one grain boundary could be affected by the neighboring boundaries, and thus the multi-sources diffusion in a finite space system can be schematically as shown in Figure 12. Nb atoms diffuse from grain boundaries into grains, and the case can be simplified as a 1D model for the short distance diffusion, and the real 3D case can be considered as diffusion in different directions which will not have an order difference in diffusion rate. For a system with many sources, if the distance between each source is 2l, the Nb concentration profile can be described as Eq. [1][26]:

$$C = \frac{1}{2} C_0 \sum_{n=-\infty}^{\infty} \left[\mathrm{erf} \frac{h - 2nl - x}{2\sqrt{Dt}} + \mathrm{erf} \frac{h - 2nl + x}{2\sqrt{Dt}} \right] \quad [1]$$

If only $n = 0, 1, -1$ are considered, the Nb concentration can be described as follows:

$$C = \frac{1}{2} C_0 \left[\operatorname{erf} \frac{h - x}{2\sqrt{Dt}} + \operatorname{erf} \frac{h + x}{2\sqrt{Dt}} + \operatorname{erf} \frac{h + 2l - x}{2\sqrt{Dt}} + \operatorname{erf} \frac{h - 2l + x}{2\sqrt{Dt}} + \operatorname{erf} \frac{h - 2l - x}{2\sqrt{Dt}} + \operatorname{erf} \frac{h + 2l + x}{2\sqrt{Dt}} \right], \quad [2]$$

where $C_0 = 0.5$ is the initial Nb concentration at boundaries, h is the half width of a grain boundary, l is the half diameter of a grain, and D is the diffusion coefficient of Nb in austenite or ferrite. The diffusion coefficient can be calculated using the typical Arrhenius equation:

$$D = D_0 \exp\left(\frac{-Q}{RT}\right). \quad [3]$$

The calculated Nb concentration profiles after various times at 1023 K (750 °C) are shown in Figure 13. In the calculation, h is chosen as 5 nm and l is chosen as 40 μm. For Nb diffusion in austenite, D_0 = 8e − 5 m^2/s and Q = 265 kJ/mol, for Nb diffusion in ferrite D_0 = 5e − 3 m^2/s and Q = 250 kJ/mol.[1]

For the sample isothermally transformed at 1023 K (750 °C), the prior austenite grain size was 80 μm and the final ferrite grain size was ~20 μm. From the dilatometer results, it is reasonable to estimate that the ferrite/austenite interface moves at an average rate of a few microns per minute at the beginning of ferrite grain growth stage during the isothermal transformation at 1023 K (750 °C). According to Figure 13, the diffusion of solute Nb atoms at this temperature is much slower than this rate. As a result, it takes extra force to 'drag' these solute Nb atoms to move with the interface, and therefore the transformation rate is slowed down. However, from the experimental observations, Nb atoms will be precipitated as Nb(C,N) particles after a few minutes holding at 1023 K (750 °C), and then the solute drag effect will be significantly reduced and the phase transformation kinetics will be much faster which is consistent with the dilatometer results as in Figure 5. From the literature,[27,28] some researchers attribute the retardation effect caused by solute Nb atoms to the increase in the activation energy of carbon diffusion, because the rate of the phase transformation from austenite to ferrite is typically controlled by carbon diffusion, and thus the ferrite grain growth rate is reduced by the presence of solute Nb atoms.

VII. CONCLUSIONS

The effects of Nb on phase transformations from austenite to ferrite have been investigated. Dilatometry results indicate that solute Nb atoms have a retardation effect on transformation kinetics from austenite to ferrite. This effect was significant on isothermal transformations above 923 K (650 °C). From microstructural analysis of interrupted isothermally transformed samples, the solute drag effect caused by many solute Nb atoms segregated at the austenite/ferrite interface has been investigated. Both ferrite nucleation rate and grain growth rate were retarded by the presence of solute Nb atoms. However, if solute Nb atoms are precipitated as Nb carbo-nitride particles before transformation, the particle pinning effect is much weaker than the solute drag effect. Solute Nb atoms also have an effect on the temperature range for reconstructive transformation, and thus the final microstructure is affected.

ACKNOWLEDGMENTS

The authors gratefully thank Tata Steel UK Limited and Loughborough University for funding this work.

REFERENCES

1. A. J. DeArdo: Proc. Int. Symp. Niobium 2001, TMS. Orlando. 2001. p. 427.
2. F. Fazeli and M. Militzer: *J. Iron Steel. Res. Int*., 2011, vol. 18 (1), pp. 658–63.
3. N. Fujita and H.K.D.H. Bhadeshia: *Mater. Sci. Technol*., 2001, vol. 17 (4), pp. 403–08.
4. J. Kim, J.G. Jung, D.H. Kim, and Y.K. Lee: *Acta Mater*., 2013, vol. 61 (19), pp. 7437–43.
5. E.G. Dere, H. Sharma, S.E. Offerman, and J. Sietsma: *Solid State Phenom*., 2011, vols. 172–174, pp. 499–504.
6. M. Gomez, S.F. Medina, A. Quispe, and P. Valles: *ISIJ Int*., 2002, vol. 42 (4), pp. 423–31.
7. C. Fossaert, G.I. Rees, T. Maurickx, and H.K.D.H. Bhadeshia: *Metall. Mater. Trans. A*, 1995, vol. 26A, pp. 21–30.
8. F. De Kazinczy, A. Axnas, and P. Pachleitner: *Jernkont Ann*, 1963, vol. 147, pp. 408–33.
9. G.I. Rees, J. Perdrix, T. Maurickx, and H.K.D.H. Bhadeshia: *Mater. Sci. Eng. A*, 1995, vol. 194, pp. 179–86.
10. S.C. Hong, S.H. Lim, K.J. Lee, D.H. Shin, and K.S. Lee: *ISIJ Int*., 2002, vol. 42 (12), pp. 1461–67.
11. J. Cao, Q. Liu, Q. Yong, and X. Sun: *J. Iron. Steel. Res. Int*., 2007, vol. 14 (3), pp. 51–55.
12. M. Gomez, S.F. Medina, and P. Valles: *ISIJ Int*., 2005, vol. 45 (11), pp. 1711–20.
13. M.G. Akben, I. Weiss, and J.J. Jonas: *Acta Metall*., 1981, vol. 29 (1), pp. 111–21.
14. S.H. Cho, K.B. Kang, and J.J. Jonas: *ISIJ Int*., 2001, vol. 41 (1), pp. 63–69.
15. Y.C. Jung, H. Ueno, H. Ohtsubo, K. Nakai, and Y. Ohmori: *ISIJ Int*., 1995, vol. 35 (8), pp. 1001–05.
16. M. Suehiro, Z.K. Liu, and J. Agren: *Acta Mater*., 1996, vol. 44 (10), pp. 4241–51.
17. M. Militzer, E.B. Hawbolt, and T.R. Meadowcroft: *Metall. Mater. Trans. A*, 2000, vol. 31A (4), pp. 1247–59.
18. L. Wang, S.V. Parker, A.J. Rose, G.D. West, and R.C. Thomson: *Metall. Mater. Trans. A*, 2000, vol. 31A (4), pp. 1247–59.
19. J.W. Cahn: *Acta Metall*., 1962, vol. 10 (9), pp. 789–98.
20. M. Hillert and B. Sundman: *Acta Metall*., 1976, vol. 24 (8), pp. 731–43.
21. G.R. Purdy and Y.J.M. Brechet: *Acta Metall. Mater*., 1995, vol. 43 (10), pp. 3763–74.
22. M. Enomoto: *Acta Mater*., 1999, vol. 47 (13), pp. 3533–40.
23. P.J. Felfer, C.R. Killmore, J.G. Williams, K.R. Carpenter, S.P. Ringer, and J.M. Cairney: *Acta Mater*., 2012, vol. 60 (13), pp. 5049–55.
24. F. Fazeli and M. Militzer: *Metall. Mater. Trans. A*, 2005, vol. 36A, pp. 1395–1405.
25. T. Furuhara, T. Yamaguchi, G. Miyamoto, and T. Maki: *Mater. Sci. Technol*., 2010, vol. 26 (4), pp. 392–97.
26. J. Crank: *The Mathematics of Diffusion*, Clarendon Press, Oxford, 1975, p. 11.
27. K.J. Lee and J.K. Lee: *Scr. Mater*., 1999, vol. 40 (7), pp. 831–36.
28. M. H. Thomas and G. M. Michal: *Proc. of Int. Conf. on Solid-Solid Phase Transform.,* TMS of AIME, Pittsburgh, 1981, p. 469.